Society of Medical Education & Research

2025, Volume 5, Issue 2, Page No: 88-106
ISSN: 3108-4826

Journal of Medical Sciences and Interdisciplinary Research

Comprehensive Evaluation and Validation of an m6A-Modulated Regulatory Pathway: The Emerging circBACH2/hsa-miR-944/HNRNPC Axis in Breast Cancer Development

Nguyen Minh Quang[1]*, Tran Thi Mai Anh[1]

[1]Department of Management, University of Economics Ho Chi Minh City, Ho Chi Minh City, Vietnam.

***E-mail** ✉ m.quang.ueh@yahoo.com

Abstract

N6-methyladenosine (m6A) represents the most prevalent and dynamic post-transcriptional alteration on messenger RNAs in eukaryotic organisms, exerting a critical influence on the initiation and advancement of breast cancer (BC). Circular RNAs (circRNAs) have the capacity to function as oncogenic drivers or inhibitors through their role as microRNA (miRNA) decoys in BC. Nevertheless, the precise pathways by which circRNAs contribute to BC development by modulating m6A regulators are not fully elucidated. m6A regulators associated with prognosis were pinpointed among 1065 BC cases drawn from The Cancer Genome Atlas (TCGA) database. Differentially expressed miRNAs and circRNAs were detected in comparisons between tumor and healthy tissues using data from TCGA and the GSE101123 dataset, respectively. Interactions between miRNAs and target mRNAs, as well as between circRNAs and miRNAs, were validated employing MiRDIP and the Circular RNA Interactome databases. Functional enrichment analyses via GSEA, KEGG pathways, and ssGSEA were performed to investigate potential biological roles and immune-related characteristics in groups stratified by high versus low HNRNPC levels. Expression levels of HNRNPC and circBACH2 in MCF-7 and MDA-MB-231 cell lines were measured using qRT-PCR and Western blotting. Cell proliferation in BC was evaluated through CCK-8 and EdU incorporation assays. Two prognostic m6A regulators, namely HNRNPC and YTHDF3, were detected in individuals with BC. Subsequently, an interaction network involving circRNAs, miRNAs, and m6A regulators was established, incorporating 2 differentially expressed m6A factors (HNRNPC and YTHDF3), 12 differentially expressed miRNAs, and 11 differentially expressed circRNAs. Of particular interest, elevated HNRNPC alongside reduced hsa-miR-944 levels in BC cases were linked to advanced disease stages and reduced overall survival. KEGG analysis further indicated that differentially expressed HNRNPC is linked to the MAPK pathway in BC. Additionally, circBACH2 (identified as hsa_circ_0001625) was validated to function as a decoy for hsa-miR-944, thereby enhancing HNRNPC levels and driving BC cell growth through the MAPK pathway, establishing a circBACH2/hsa-miR-944/HNRNPC regulatory pathway in BC. This research uncovers a distinctive m6A modulation mechanism mediated by circRNAs that contributes to BC advancement, offering promising avenues for improved diagnosis and treatment approaches in BC management.

Keywords: Breast cancer, Circular RNA, MicroRNA, m6A RNA methylation modulator

Introduction

Breast cancer (BC) stands as the leading malignant tumor among women and a primary contributor to cancer-associated deaths in the United States [1]. Although advancements in detection methods and treatments for BC have occurred over recent years, patient outcomes and extended survival rates continue to be suboptimal, largely due to the disease's molecular diversity, pronounced tendency for metastasis, and challenges in early identification [2]. Consequently, discovering novel molecular indicators with greater accuracy and reliability for BC screening and therapy is essential.

N6-methyladenosine (m6A) alteration involves adding a methyl group to the sixth nitrogen of adenosine in mRNA and is the most common, widespread, and evolutionarily maintained internal modification during transcription in

Access this article online https://smerpub.com/

Received: 23 June 2025; **Accepted:** 14 October 2025

How to cite this article: Quang NM, Anh TTM. Comprehensive Evaluation and Validation of an m6A-Modulated Regulatory Pathway: The Emerging circBACH2/hsa-miR-944/HNRNPC Axis in Breast Cancer Development. J Med Sci Interdiscip Res. 2025;5(2):88-106. https://doi.org/10.51847/ZJFPwvb6zd

eukaryotes. The effects of m6A on RNA fate are governed by reversible interplay among m6A regulators, encompassing methyltransferases (writers), recognition proteins (readers), and demethylases (erasers) [3]. Typically, m6A is added by a methyltransferase complex acting as writers, including METTL3, METTL14, RBM15, and ZC3H13 [4]. Erasers like FTO, ALKBH3, and ALKBH5 can reverse this modification to maintain equilibrium between methylation and removal [5]. Moreover, the dynamic nature of m6A also relies on detection by reader proteins, primarily the YTH domain family [6, 7]. Growing data suggest that m6A changes are intimately involved in cancer development, including cell growth, differentiation, invasion, and unfavorable outcomes [8]. The writers, erasers, and readers associated with m6A participate in BC onset and progression. Such BC-related m6A factors hold potential as markers for prognosis and targeted interventions.

Circular RNAs (circRNAs) are non-linear RNA structures formed by covalent closure without 5' caps or 3' poly-A tails, produced through back-splicing events [9]. In BC, circRNAs frequently serve as oncogenes or tumor suppressors primarily by sequestering miRNAs. Recent investigations have also highlighted circRNAs acting as miRNA decoys to influence m6A regulators in cancers such as liver [10], stomach [11], and adrenocortical tumors [12]. Yet, comprehensive examinations of circRNA-m6A interactions in BC are limited. Mapping circRNA networks tied to m6A regulators could yield vital insights into mechanisms and novel targets for BC therapy.

In this investigation, we screened for prognostic differentially expressed m6A regulators, circRNAs, and miRNAs in BC versus adjacent normal samples from TCGA and GEO repositories, followed by building a circRNA-miRNA-mRNA interaction framework. Drawing from clinical data and miRNA-m6A co-expression trends, we inferred that elevated hsa-miR-944 combined with reduced HNRNPC correlates with improved survival in BC compared to counterparts. Critically, circBACH2 (hsa_circ_0001625) was experimentally shown to facilitate BC cell growth by sequestering hsa-miR-944 and thereby upregulating HNRNPC. Furthermore, the circBACH2/hsa-miR-944/HNRNPC pathway promoted BC advancement in a MAPK pathway-reliant fashion. These observations illuminate novel ways circRNAs control m6A regulators via miRNA binding, opening fresh opportunities for diagnostic and therapeutic advancements in BC.

Materials and Methods

Acquisition and preprocessing of breast cancer datasets

High-throughput RNA sequencing (RNA-seq), miRNA sequencing (miRNA-seq), and matched clinicopathological information for breast cancer (BC) patients were retrieved from The Cancer Genome Atlas (TCGA) repository (https://portal.gdc.cancer.gov/) and prepared for downstream differential expression and co-expression analyses. Samples lacking survival outcome data were excluded from prognostic evaluations. The survival relevance of miRNAs and m6A RNA methylation regulators was independently validated using datasets from TCGA, the Gene Expression Omnibus (GEO; https://www.ncbi.nlm.nih.gov/geo/), and the Tang_2018 cohort available through KM-plotter (http://kmplot.com/analysis/index.php?p=background). CircRNA expression profiles were obtained from the GEO dataset GSE101123.

Screening of differentially expressed (DE) genes

Based on prior publications, 21 known m6A methylation regulators were initially curated [3, 13]. Using TCGA mRNA expression data, 17 regulators exhibiting differential expression between 1065 BC tissues and 112 normal controls were identified via the Mann–Whitney–Wilcoxon test. The prognostic significance of these m6A regulators was subsequently examined using univariate Cox proportional hazards analysis followed by LASSO-Cox regression, and the differentially expressed prognostic regulators were retained for subsequent network construction. Differential miRNA expression between 1057 BC samples and 103 normal tissues in TCGA was assessed using the “limma” package from Bioconductor. Adjusted P values were calculated with the Benjamini–Hochberg procedure to control the false discovery rate (FDR), and miRNAs meeting FDR < 0.05 with |log2 fold change (FC)| > 1 were considered significant. Differentially expressed circRNAs between 8 BC samples and 3 normal samples in GSE101123 were determined using a rank aggregation strategy. The identified DE miRNAs and circRNAs were visualized using heatmap representations.

Establishment of the circRNA–miRNA–m6A regulator interaction network

Putative miRNA–m6A RNA methylation regulator interactions were predicted using the miRDIP platform (http://ophid.utoronto.ca/mirDIP/), whereas circRNA–

miRNA associations were obtained from the Circular RNA Interactome database (https://circinteractome.nia.nih.gov/). For miRNA–m6A regulator pairing, only miRNAs predicted with very high confidence (top 1% score) in miRDIP and concurrently identified as DE miRNAs in BC tissues from TCGA were retained. The final circRNA–miRNA–mRNA regulatory network was constructed by intersecting the filtered miRNA–m6A regulator interactions with the circRNA–miRNA interaction dataset.

Gene set enrichment analysis (GSEA), Kyoto Encyclopedia of Genes and Genomes (KEGG) analysis, and single-sample GSEA (ssGSEA)

A total of 1178 TCGA BC samples were stratified into high- and low-expression groups according to HNRNPC expression levels. These groups were subjected to GSEA (http://software.broadinstitute.org/gsea/index.jsp) to identify enriched biological processes and pathways associated with differential HNRNPC expression. The reference gene sets included c5.go.bp.v7.4.symbols.gmt, c5.go.cc.v7.4.symbols.gmt, c5.go.mf.v7.4.symbols.gmt, and c2.cp.kegg.v7.4.symbols.gmt, with significance defined as nominal $P < 0.05$. In line with previously reported evidence [14–16], BC-related biological processes and signaling pathways were selectively visualized. KEGG pathway enrichment analysis comparing HNRNPC high- and low-expression groups was conducted using R software (version 4.0.1). To further explore the potential immunomodulatory role of HNRNPC in BC, the "gsva" R package was applied to perform ssGSEA, enabling the quantification of immune cell infiltration scores and the functional activity of immune-associated pathways.

Cell culture conditions and transfection procedures

Human BC cell lines MCF-7 and MDA-MB-231 were purchased from the American Type Culture Collection (ATCC; Manassas, VA, USA). Cells were maintained in Dulbecco's Modified Eagle's Medium (DMEM) supplemented with 10% (v/v) fetal bovine serum (Gibco) and incubated at 37 °C in a humidified atmosphere containing 5% CO_2. Small interfering RNAs targeting HNRNPC and circBACH2, hsa-miR-944 inhibitors, and their respective negative controls were obtained from RiboBio (Wuhan, China). Cells were seeded into six-well plates and transfected with 50 nM siRNA or inhibitor using Lipofectamine 3000 (Invitrogen), following the manufacturer's protocol. All transfection experiments were independently repeated three times.

Assessment of cell proliferation

Cell proliferation was evaluated using both the Cell Counting Kit-8 (CCK-8; Dojindo, Kumamoto, Japan) and the 5-ethynyl-2′-deoxyuridine (EdU) incorporation assay (RiboBio, Wuhan, China). For the CCK-8 assay, transfected cells were plated in 96-well plates at a density of 2×10^3 cells per well. Cell viability was monitored at intervals ranging from 12 to 72 h following transfection by adding CCK-8 reagent directly to the wells, and absorbance was measured at 450 nm using a microplate reader (BioTek Instruments, USA). For the EdU assay, BC cells were exposed to culture medium containing 50 μM EdU for 2 h, fixed with 4% paraformaldehyde for 30 min, and subsequently stained with Apollo reaction solution and Hoechst 33,342. Proliferative activity was quantified as the proportion of EdU-positive cells relative to the total DAPI-stained cell population under a fluorescence microscope (IX35, Olympus, Japan). Each assay was performed in triplicate.

Quantitative real-time PCR (qRT-PCR)

Total RNA was extracted from BC cells using TRIzol reagent (Invitrogen). RNA concentration and purity were determined with a NanoDrop 2000 spectrophotometer (Thermo Fisher Scientific, Wilmington, DE, USA). Complementary DNA (cDNA) synthesis was carried out using the PrimeScript RT kit (Takara, Japan) under the following conditions: 103 °C for 5 s, 37 °C for 10 min, and 4 °C for 15 min. GAPDH served as the internal reference gene. Relative gene expression levels were calculated using the $2^{-\Delta\Delta Ct}$ method. All qRT-PCR analyses were conducted across three independent experimental replicates.

Western blot analysis

Total cellular proteins were isolated using radioimmunoprecipitation assay (RIPA) buffer (Boster, Wuhan, China), and protein concentrations were quantified with a bicinchoninic acid (BCA) assay kit (Boster, Wuhan, China). Equal amounts of protein were separated on 10% sodium dodecyl sulfate–polyacrylamide gels (SDS–PAGE), initially run at 80 V for 20 min followed by 120 V for 1 h, and subsequently electrotransferred onto polyvinylidene difluoride (PVDF) membranes (Biosharp, Shanghai, China) at 220 mA for 60 min. Membranes were washed multiple times

with Tris-buffered saline containing Tween 20 (TBST) and blocked with 5% bovine serum albumin (BSA) at 37 °C for 2 h. They were then incubated overnight at 4 °C with primary antibodies against HNRNPC (1:4000), GAPDH (1:5000), phosphorylated ERK (p-ERK, 1:1500), total ERK (t-ERK, 1:1500), total MAPK (t-MAPK, 1:1000), and phosphorylated MAPK (p-MAPK, 1:1500). Afterward, membranes were exposed to horseradish peroxidase (HRP)-conjugated secondary antibodies (1:5000; Abcam, Cambridge, MA, United States) for 1 h at 37 °C. Protein signals were detected using an enhanced chemiluminescence (ECL) system (Yeasen, Shanghai, China), and band intensities were quantified using ImageJ software (version 1.44p, National Institutes of Health, United States). All primary antibodies were obtained from Proteintech (Wuhan, China).

Statistical analysis

All statistical computations were performed using R software (version 4.0.5) and GraphPad Prism (version 8.0). Differences in m6A RNA methylation regulator expression between tumor and normal tissues were analyzed using the Mann–Whitney U test. Comparisons between two defined subgroups were conducted with Student's t-test. Univariate and multivariate Cox proportional hazards regression models were applied to evaluate independent prognostic factors and their associations with clinical variables. Pearson correlation coefficients were calculated to assess relationships between continuous variables. A two-sided P value < 0.05 was considered indicative of statistical significance.

Results and Discussion

Upregulation of m6A RNA methylation regulators in breast cancer

The overall analytical workflow is illustrated in **Figure 1**. Within the TCGA cohort, expression profiles of 17 m6A RNA methylation regulators were systematically compared between 1065 BC tissues and 112 non-tumor samples. Among these regulators, 12 genes displayed significantly elevated expression levels in BC, whereas the remaining 5 genes did not show statistically meaningful differences **(Figures 2a and 2b).** These findings suggest that m6A regulatory factors present distinct expression patterns in BC compared with normal tissues and may hold diagnostic relevance. Interrelationships among the 17 m6A regulators were further depicted using a correlation heatmap **(Figure 2c).** Subsequently, the prognostic relevance of m6A RNA methylation modulators was examined using TCGA survival data. Univariate Cox regression analysis revealed that RBM15B functioned as a protective factor associated with improved overall survival in BC patients, whereas elevated expression of HNRNPC and YTHDF3 correlated with poorer survival outcomes **(Figure 2d)**. Further refinement through LASSO regression and stepwise multivariate Cox analysis identified a prognostic signature consisting of four m6A regulators—RBM15B, HNRNPC, YTHDF3, and ZC3H13—for BC risk stratification **(Figures 2e and 2f)**. Consistently, forest plot analysis demonstrated that higher expression levels of HNRNPC, YTHDF3, and ZC3H13 were significantly associated with adverse overall survival in BC patients **(Figure 2f)**. Based on these results, subsequent analyses primarily concentrated on the prognostically unfavorable m6A RNA methylation regulators in BC, particularly HNRNPC and YTHDF3.

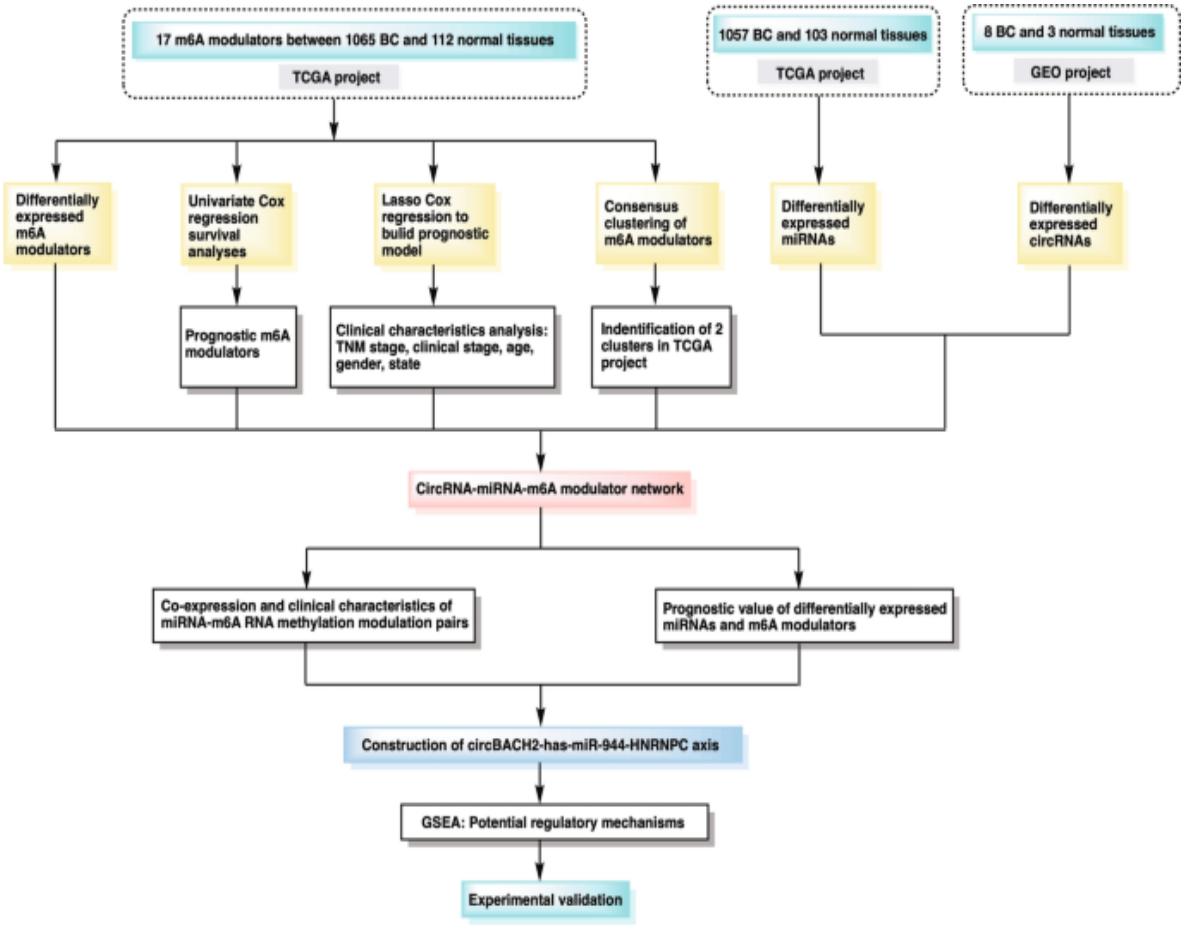

Figure 1. Schematic overview outlining the overall design, analytical workflow, and sequential steps of the study.

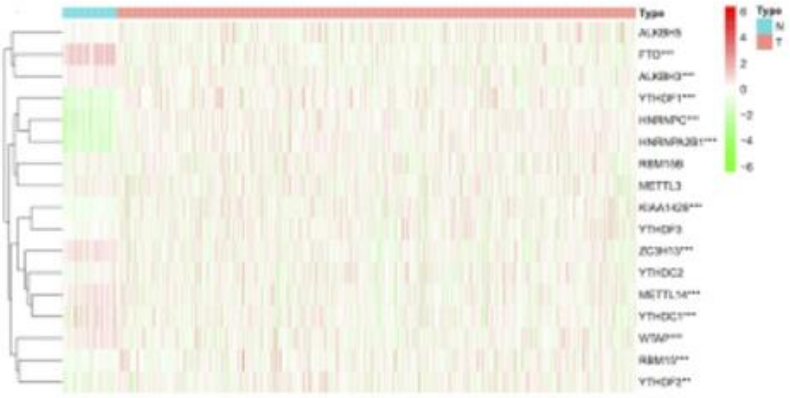

a)

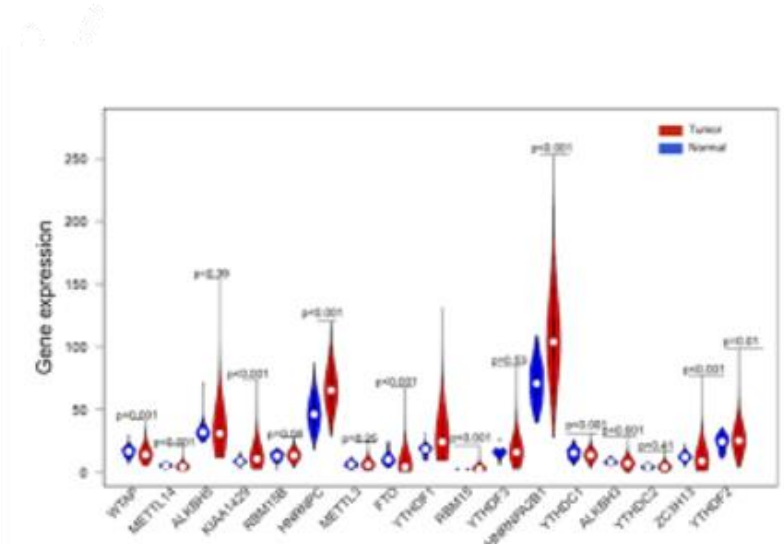

b)

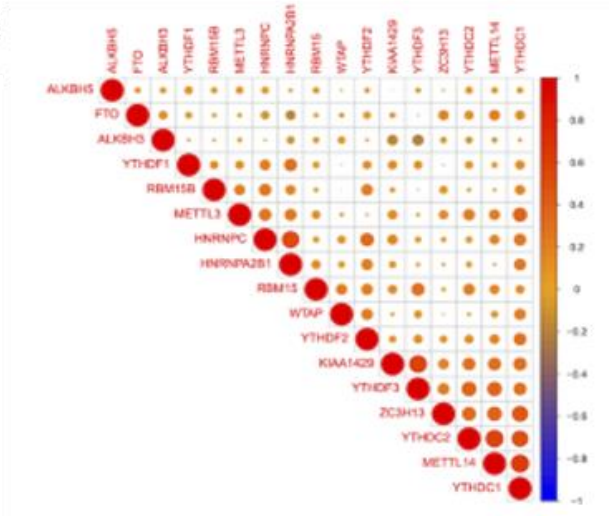

c)

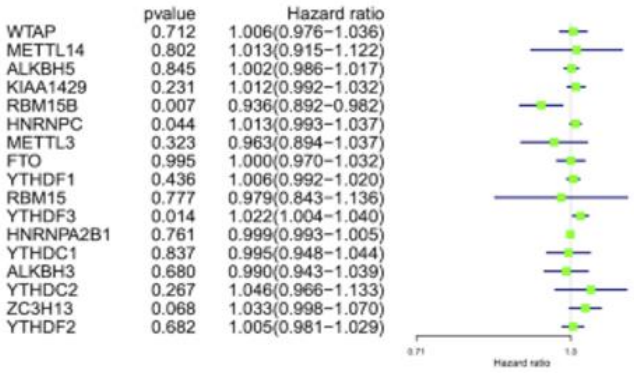

	pvalue	Hazard ratio
WTAP	0.712	1.006(0.976−1.036)
METTL14	0.802	1.013(0.915−1.122)
ALKBH5	0.845	1.002(0.986−1.017)
KIAA1429	0.231	1.012(0.992−1.032)
RBM15B	0.007	0.936(0.892−0.982)
HNRNPC	0.044	1.013(0.993−1.037)
METTL3	0.323	0.963(0.894−1.037)
FTO	0.995	1.000(0.970−1.032)
YTHDF1	0.436	1.006(0.992−1.020)
RBM15	0.777	0.979(0.843−1.136)
YTHDF3	0.014	1.022(1.004−1.040)
HNRNPA2B1	0.761	0.999(0.993−1.005)
YTHDC1	0.837	0.995(0.948−1.044)
ALKBH3	0.680	0.990(0.943−1.039)
YTHDC2	0.267	1.046(0.966−1.133)
ZC3H13	0.068	1.033(0.998−1.070)
YTHDF2	0.682	1.005(0.981−1.029)

d)

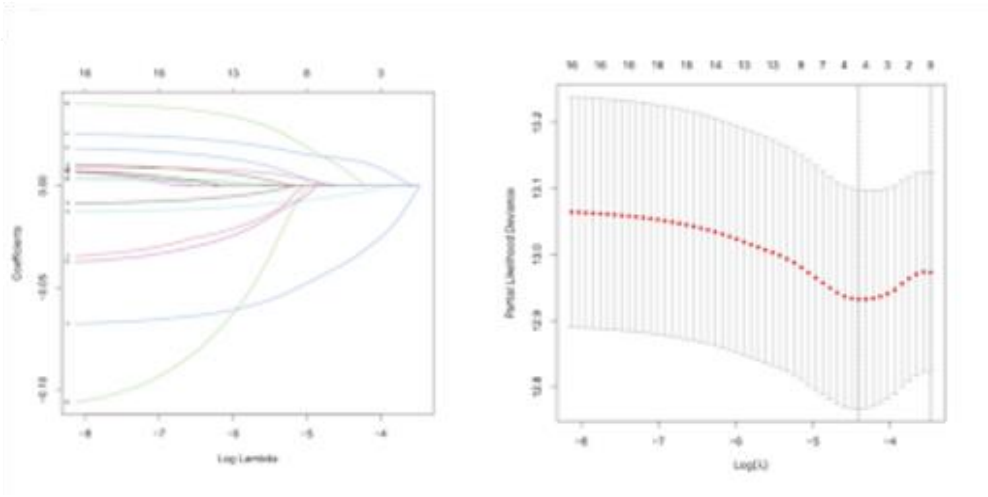

e)

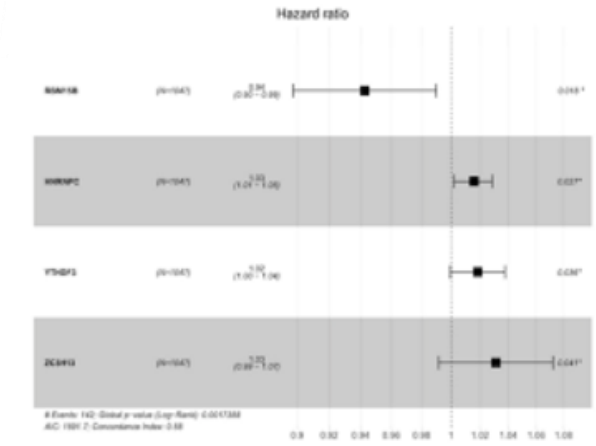

f)

Figure 2. Expression patterns, prognostic relevance, and construction of an m6A-related risk model in breast cancer. (a) Heatmap illustrating the expression profiles of 17 prognostically relevant m6A regulators in the TCGA cohort. Statistical significance is indicated by asterisks (**P < 0.01; ***P < 0.001). (b) Comparative expression analysis of the 17 m6A regulators between breast cancer tissues and normal controls in TCGA (tumor samples shown in red; normal samples in blue). (c) Pearson correlation matrix demonstrating the relationships among the m6A regulators. (d) Univariate Cox proportional hazards analysis evaluating the association between m6A RNA methylation modulators and overall survival (OS) in TCGA breast cancer patients. (e) LASSO Cox regression analysis applied to the 17 m6A-associated genes. (f) Forest plot depicting hazard ratios for the association between four differentially expressed m6A regulators and OS in breast cancer patients.

circRNA–miRNA–m6A RNA methylation modulator regulatory network in breast cancer

Subsequently, differential expression analysis identified 154 circRNAs (96 upregulated and 58 downregulated) between breast cancer and normal samples in the GSE101123 dataset, as well as 377 differentially expressed miRNAs in TCGA breast cancer samples, including 268 upregulated and 109 downregulated miRNAs **(Figure 3A).** Among these, the most prominent candidates—27 circRNAs (34 upregulated and 18 downregulated) **(Figure 3b)** and 30 miRNAs (9 upregulated and 21 downregulated)—were selected for heatmap visualization.

Interaction prediction analysis yielded 271 potential miRNA–m6A RNA methylation regulator pairs and 1680 putative circRNA–miRNA interactions. By intersecting these datasets, two key m6A regulators (HNRNPC and YTHDF3), together with 12 differentially expressed miRNAs and 11 differentially expressed circRNAs, were retained to establish the regulatory framework. The final circRNA–miRNA–m6A RNA methylation modulator network comprised 16 circRNA–miRNA interaction pairs and 13 miRNA–mRNA interaction pairs, as illustrated in **Figure 3c**.

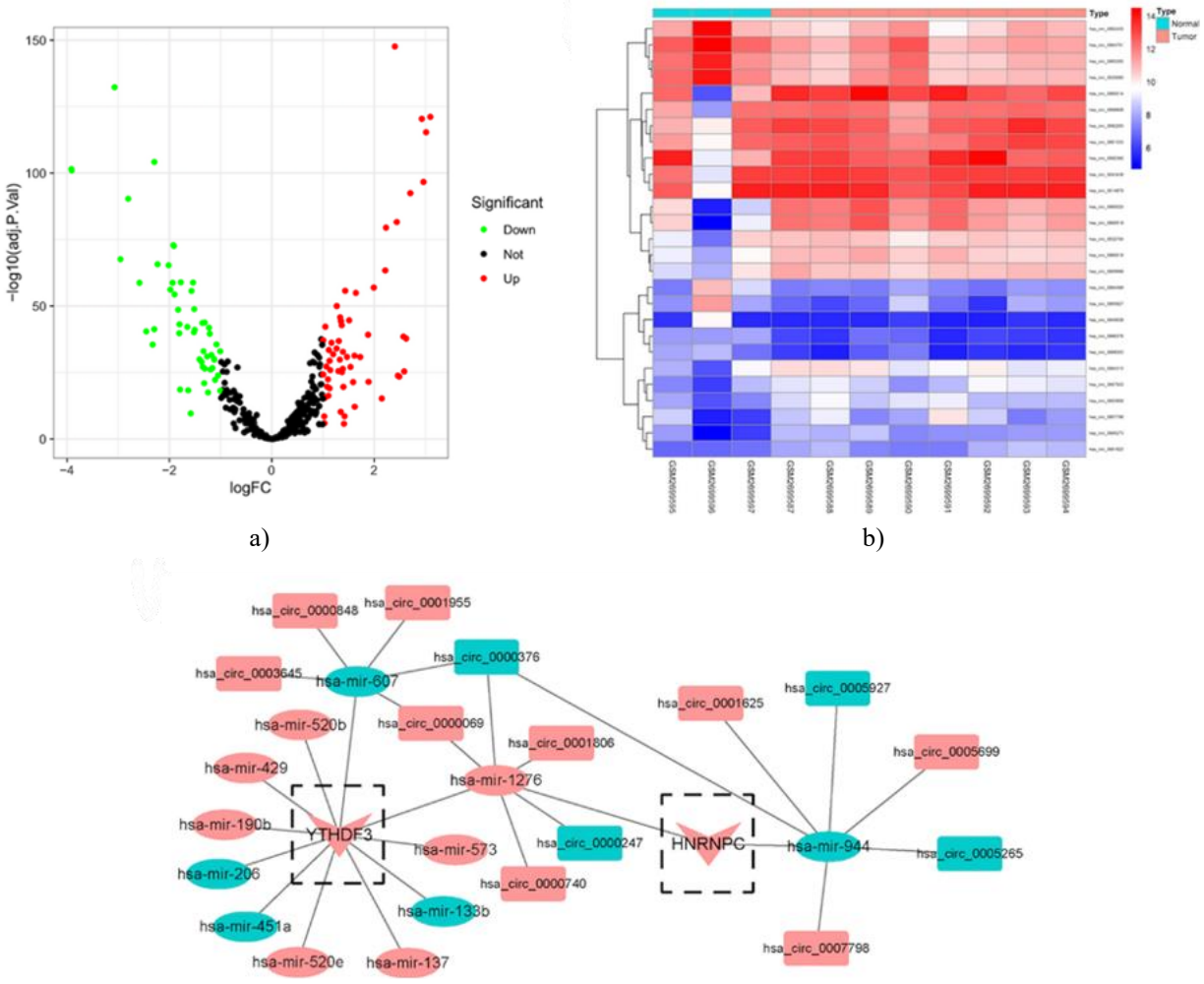

a) b)

c)

Figure 3. Identification of differentially expressed (DE) miRNAs and circRNAs and construction of the regulatory network.

(a) Volcano plot displaying 377 DE miRNAs in the TCGA cohort.

(b) Heatmap illustrating 27 significant DE circRNAs in GSE101123.

(c) circRNA–miRNA–mRNA regulatory network. Rectangles, ovals, and triangles represent circRNAs, miRNAs, and mRNAs, respectively; red indicates upregulation and green indicates downregulation

Co-expression analysis and clinical correlations of miRNA–m6A RNA methylation modulator pairs

To identify the most relevant miRNA–mRNA interactions, Pearson correlation analysis was performed between five DE miRNAs and two m6A RNA methylation regulators. As shown in **Figure 4a**, five co-expressed miRNA–m6A regulator pairs were detected, with hsa-miR-944 exhibiting a significant negative correlation with HNRNPC ($r = -0.139$, $P < 0.001$). Consistently, hsa-miR-944 was downregulated in BC

tissues compared with normal tissues across three GEO datasets, whereas HNRNPC was upregulated in BC tissues in four GEO datasets, confirming a potential inverse relationship between hsa-miR-944 and HNRNPC.

Further analysis evaluated associations between the two m6A regulators and five DE miRNAs with clinical BC stages and TNM classifications. Notably, elevated HNRNPC expression was significantly associated with advanced clinical stage III as well as late T and N stages **(Figure 4b).** In contrast, YTHDF3 expression did not show significant correlations with clinical stage or TNM stages **(Figure 4c)**. Among the five DE miRNAs, only high hsa-miR-944 expression correlated significantly with early clinical stage I and T stage ($P < 0.05$), while no significant associations were observed for N or M stages **(Figure 4d)**. Collectively, these findings suggest that the hsa-miR-944–HNRNPC pair represents the most clinically relevant interaction in BC. C.

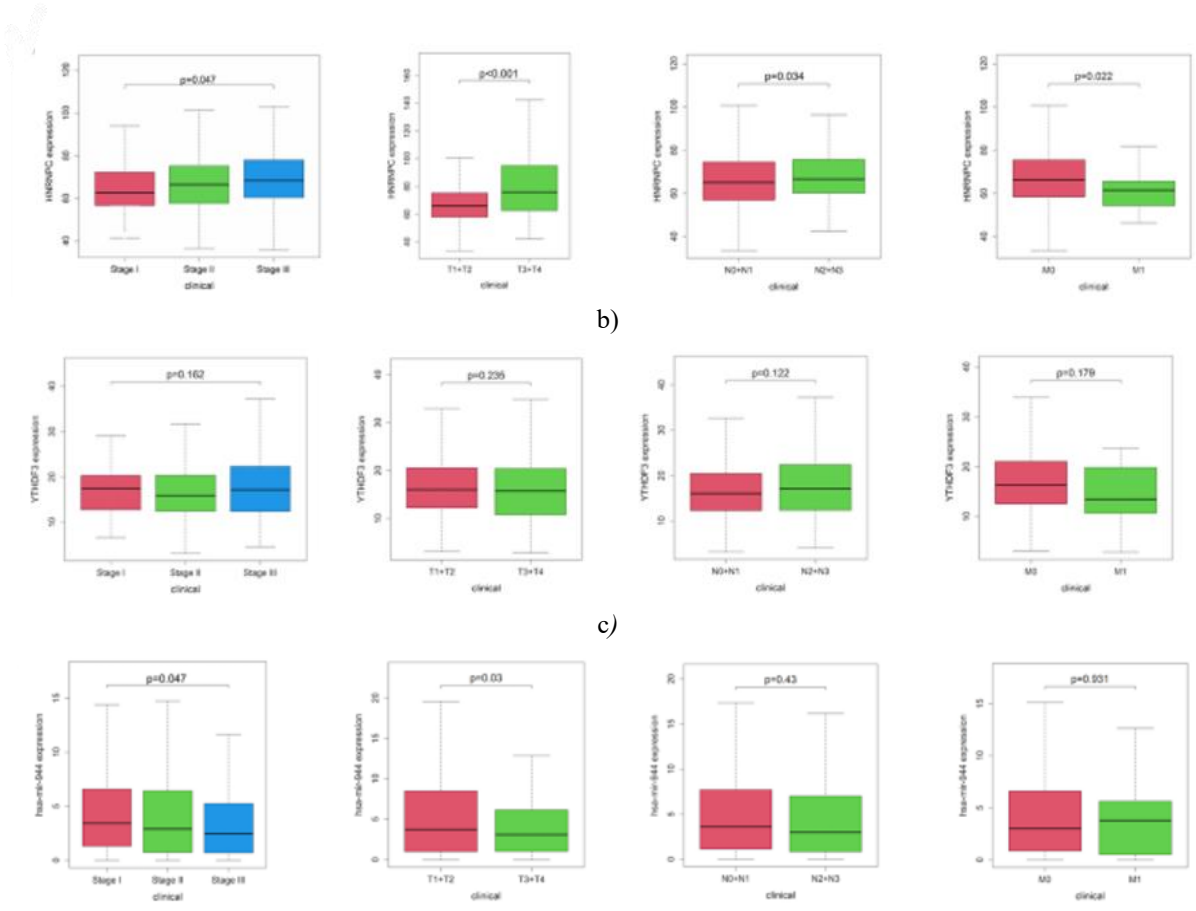

Figure 4. Co-expression patterns and clinical correlations of miRNAs and m6A RNA methylation modulators in the TCGA cohort.

(a) Pearson correlation analysis between five DE miRNAs and two m6A regulators.

(b–d) Associations of HNRNPC (B), YTHDF3 (c), and hsa-miR-944 (d) expression levels with clinical stages and TNM classifications in breast cancer patients.

Prognostic significance of hsa-miR-944 and HNRNPC and construction of the circRNA–hsa-miR-944–HNRNPC regulatory network

Survival analyses demonstrated that high hsa-miR-944 expression predicted favorable prognosis and prolonged overall survival (OS) in BC patients ($P < 0.05$) **(Figure 5a),** whereas elevated HNRNPC expression was associated with shorter OS ($P < 0.001$) **(Figure 5b).** The prognostic relevance of HNRNPC was further confirmed in the GSE11121 **(Figure 5c)** and Tang_2018 datasets

(Figure 5d), showing trends consistent with TCGA findings. Considering the heterogeneity of BC, the prognostic value of HNRNPC was assessed across five molecular subtypes. Except for luminal A ($P > 0.05$), high HNRNPC expression correlated with poor prognosis in basal-like, HER2-positive, luminal B, and normal-like BC subtypes ($P < 0.05$) **(Figures 5e–5h).**

Based on the co-expression patterns of miRNA–m6A regulator pairs, it was inferred that low hsa-miR-944 expression combined with high HNRNPC expression contributes to BC progression. Consistently, patients exhibiting this expression pattern had significantly shorter OS compared to patients with opposite expression levels **(Figure 5i).** Specifically, reduced OS was particularly observed in basal-like and luminal B BC patients with high HNRNPC and low hsa-miR-944 expression.

Accordingly, a prognostically relevant circRNA–miRNA–mRNA regulatory network was constructed based on HNRNPC and hsa-miR-944, comprising six regulatory axes: hsa_circ_0000376/hsa-miR-944/HNRNPC, hsa_circ_0001625/hsa-miR-944/HNRNPC, hsa_circ_0005927/hsa-miR-944/HNRNPC, hsa_circ_0005699/hsa-miR-944/HNRNPC, hsa_circ_0005265/hsa-miR-944/HNRNPC, and hsa_circ_0007798/hsa-miR-944/HNRNPC **(Figure 5j).**

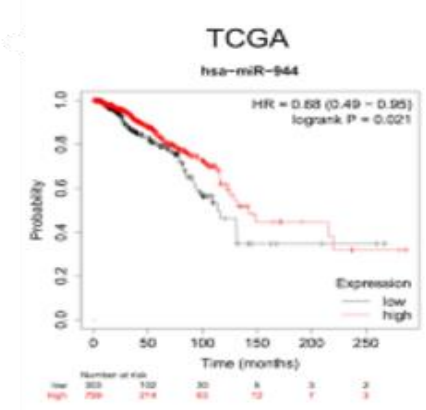

a)

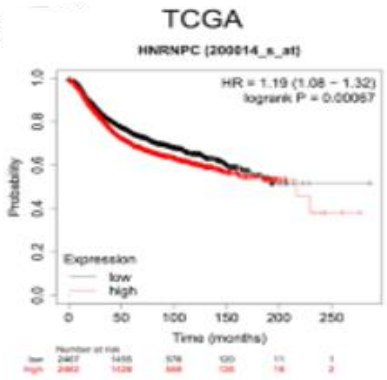

b)

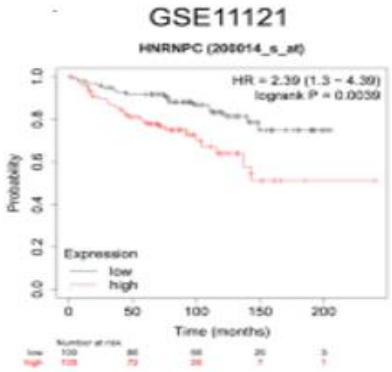

c)

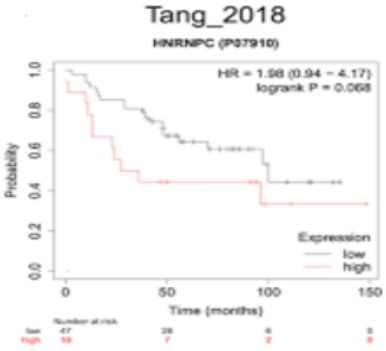

d)

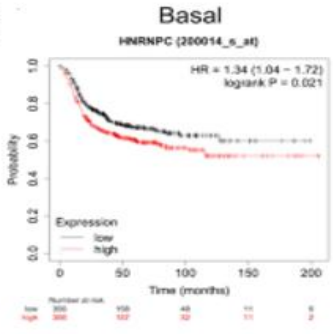

e)

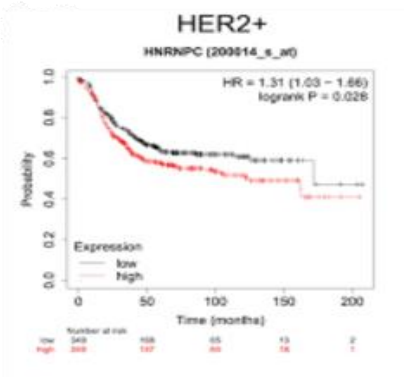

f)

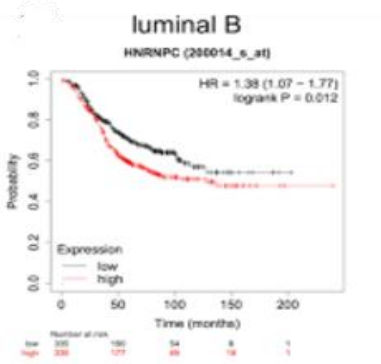

g)

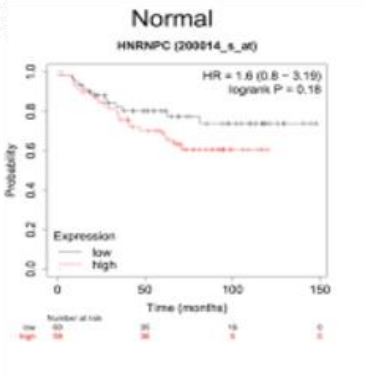

h)

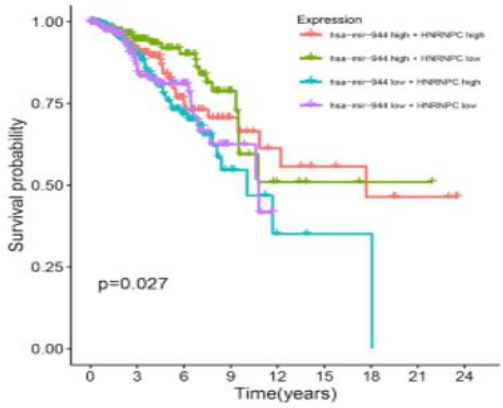

i)

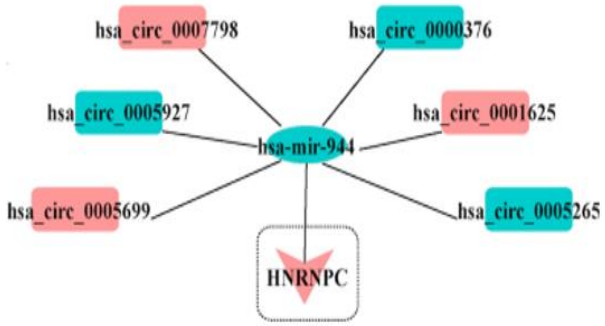

j)

Figure 5. Prognostic significance of HNRNPC and hsa-miR-944 and construction of the core circRNA–hsa-miR-944–HNRNPC regulatory network in breast cancer.

(a) Kaplan–Meier survival curves for BC patients stratified by high versus low hsa-miR-944 expression.

(b–d) Kaplan–Meier survival analyses of BC patients with high and low HNRNPC expression in the TCGA cohort (B), GSE11121 dataset (c), and Tang_2018 cohort (d).

(e–h) Kaplan–Meier survival analyses for BC subtypes with high and low HNRNPC expression: basal-like (e), HER2-positive (f), luminal B-like (g), and normal-like (Hh).

(i) Kaplan–Meier survival analysis of BC patients based on combined expression patterns of hsa-miR-944 and HNRNPC in TCGA.

(j) Construction of the core circRNA–hsa-miR-944–HNRNPC regulatory network. Rectangles, ovals, and triangles indicate circRNAs, miRNAs, and mRNAs, respectively; red and green indicate upregulation and downregulation.

Potential regulatory mechanisms in HNRNPC differential expression groups

Gene set enrichment analysis (GSEA) revealed that HNRNPC high-expression groups were enriched for processes related to gene expression and mRNA stability, including nucleotide excision repair, RNA splicing, and RNA polymerase complex activity, highlighting the functional impact of m6A modifications in eukaryotic cells **(Figures 6a–6c)**. KEGG pathway analysis further indicated that low HNRNPC expression was significantly associated with tumor-related pathways such as JAK/STAT and MAPK signaling, whereas high HNRNPC expression correlated with cell cycle–related processes ($P < 0.05$) **(Figure 6d)**. These results suggest

that altered HNRNPC expression may influence BC progression via modulation of the cell cycle, JAK/STAT, and MAPK pathways.

Moreover, single-sample GSEA (ssGSEA) quantified enrichment scores for 16 immune cell types and 13 immune-related functions, revealing distinct differences in immune cell infiltration and functional activity between high and low HNRNPC expression groups **(Figures 6e and 6f)**. These findings provide a basis for future investigations into the potential role of HNRNPC in tumor immunity in BC.

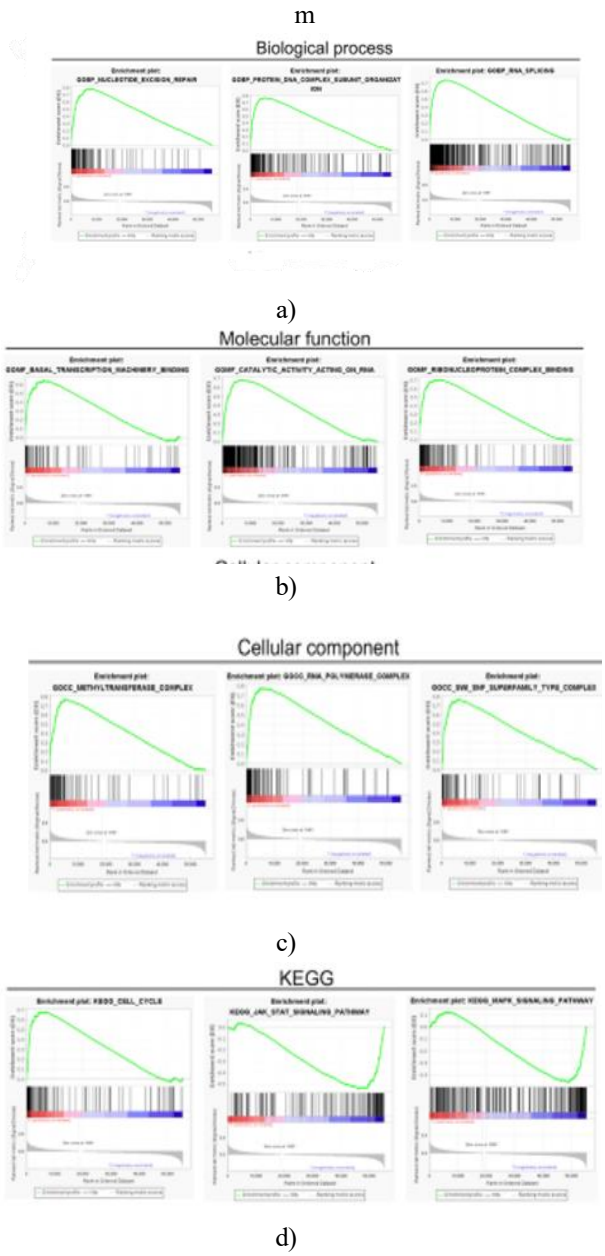

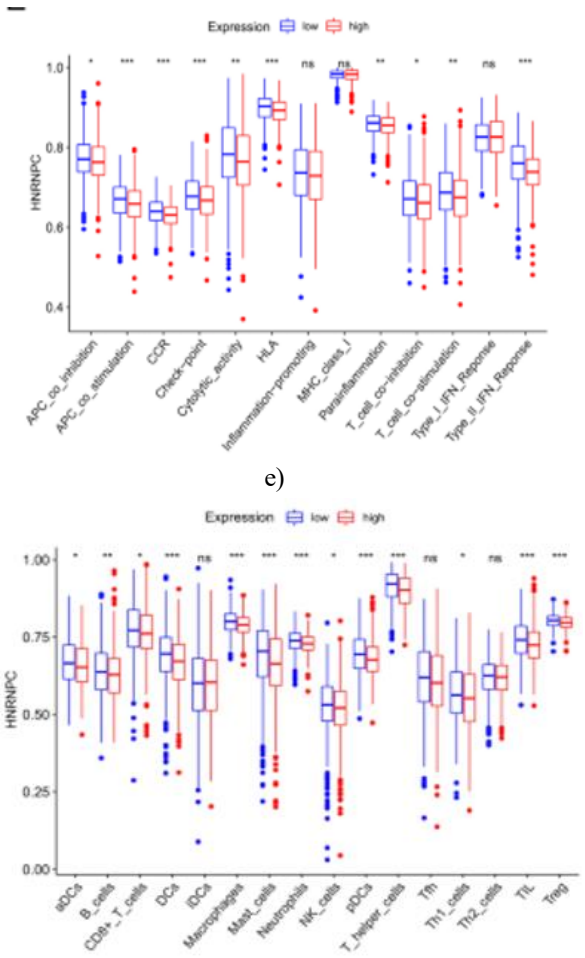

Figure 6. GSEA, KEGG, and ssGSEA analyses comparing HNRNPC high- and low-expression groups in breast cancer from the TCGA cohort.

(a–c) Functional enrichment analyses between HNRNPC high and low expression groups: biological processes (a) including nucleotide excision repair, protein-DNA complex subunit organization, and RNA splicing; molecular functions (b) including basal transcription machinery binding, catalytic activity acting on RNA, and ribonucleoprotein complex binding; and cellular components (c) including methyltransferase complex, RNA polymerase complex, and SWI-SNF superfamily-type complex.

(d) KEGG pathway analysis showing differentially enriched pathways between HNRNPC high and low expression groups.

(e, f) ssGSEA analyses showing enrichment scores of 16 immune cell types (e) and 13 immune-related functions (f) between HNRNPC high and low expression groups.

CircBACH2 promotes breast cancer cell proliferation via the hsa-miR-944/HNRNPC axis

Among six dysregulated circRNAs identified as regulators of BC progression and prognosis through the hsa-miR-944/HNRNPC axis, circBACH2 (hsa_circ_0001625) exhibited the highest interaction score with hsa-miR-944 according to Circular RNA Interactome (https://circinteractome.nia.nih.gov/). Previous studies also linked circBACH2 to progression in multiple cancers, including triple-negative breast cancer (TNBC) [17] and papillary thyroid carcinoma (PTC) [18], supporting its selection for further functional analysis in BC.

Cell transfection experiments demonstrated that siRNA-mediated knockdown of HNRNPC effectively reduced its RNA and protein expression in MDA-MB-231 and MCF-7 cells **(Figures 7a–7c).** Correspondingly, HNRNPC silencing significantly inhibited proliferation of these cells as measured by CCK-8 assay. Similarly, circBACH2 knockdown suppressed proliferation in MDA-MB-231 and MCF-7 cells **(Figures 7d and 7f)** and decreased the proportion of EdU-positive cells, indicating its role in promoting cell proliferation **(Figure 7e and 7g)**.

To explore the regulatory mechanism, the effect of circBACH2 on the hsa-miR-944/HNRNPC axis was examined. Transfection with a hsa-miR-944 inhibitor increased HNRNPC RNA and protein levels in both cell lines, whereas circBACH2 knockdown reversed these effects **(Figures 8a–8c)**, confirming the modulation of HNRNPC by the circBACH2–hsa-miR-944 network. Functional assays further revealed that hsa-miR-944 inhibition enhanced BC cell proliferation, but this stimulatory effect was partially abolished by circBACH2 silencing **(Figures 8d–8g)**. Collectively, these results indicate that circBACH2 acts as a sponge for hsa-miR-944, regulating HNRNPC expression and activity, thereby promoting breast cancer cell proliferation.

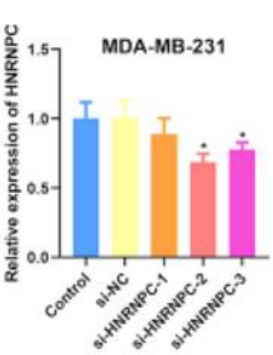

a)

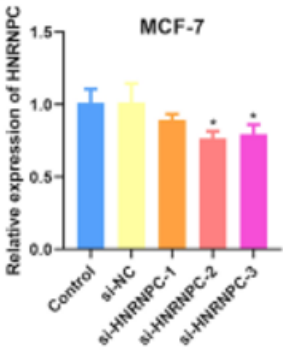

b)

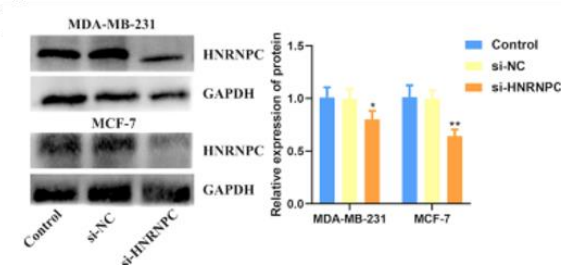

c)

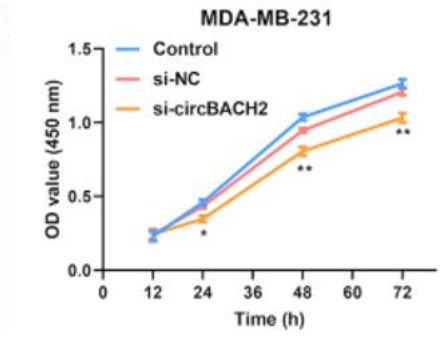

d)

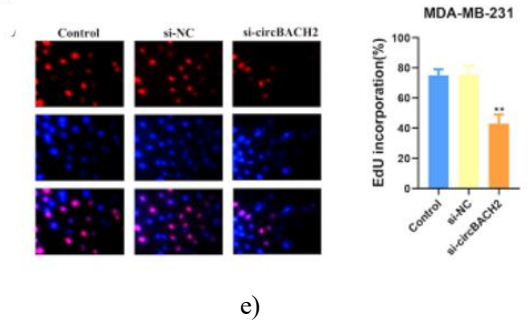

e)

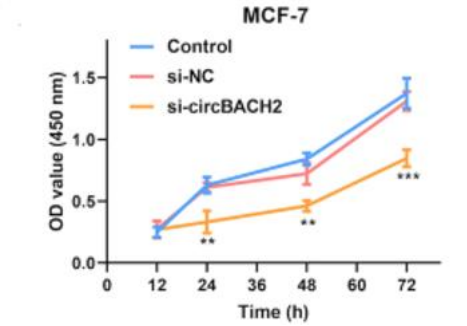

f)

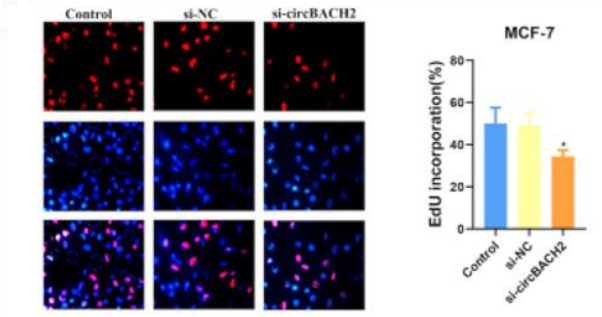

g)

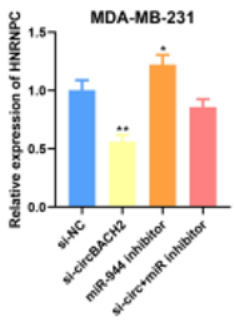

a)

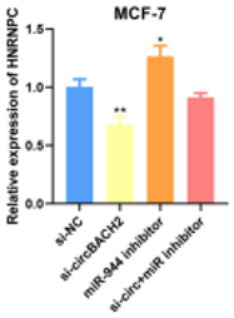

b)

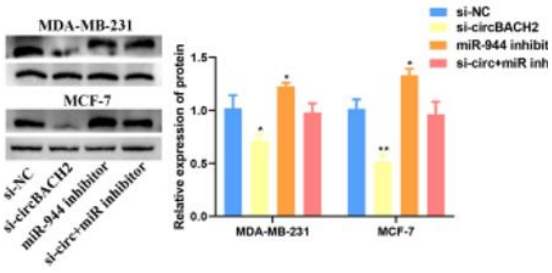

c)

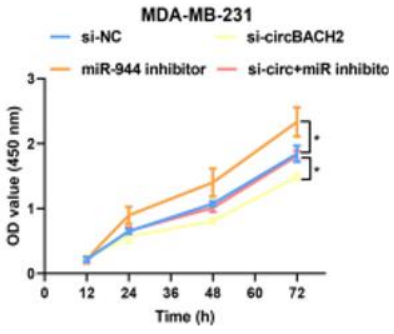

d)

Figure 7. circBACH2 and HNRNPC enhance proliferation of breast cancer cells.
(a, b) Relative HNRNPC mRNA levels in MDA-MB-231 (a) and MCF-7 (b) cells measured by qRT-PCR after silencing HNRNPC with siRNA.
(c) Protein expression of HNRNPC in both MDA-MB-231 and MCF-7 cells following circBACH2 knockdown, assessed by Western blot.
(d, f) Cell proliferation measured by CCK-8 assay in MDA-MB-231 (d) and MCF-7 (f) cells after transfection with circBACH2-specific siRNAs or negative controls.
(e, g) EdU incorporation assay showing the proportion of proliferating MDA-MB-231 (e) and MCF-7 (g) cells after circBACH2 depletion compared with control.
*P < 0.05 compared with siRNA negative control.

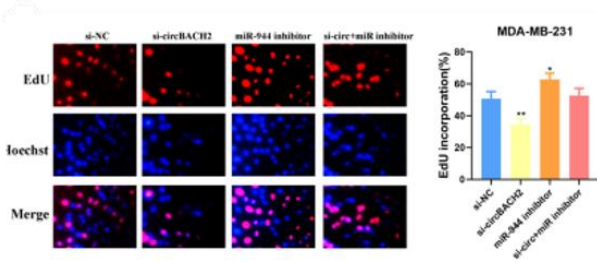

e)

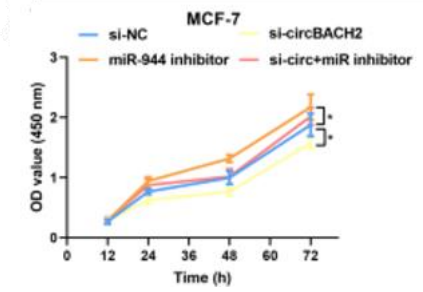

f)

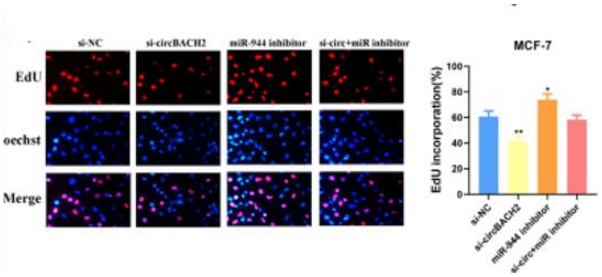

g)

Figure 8. circBACH2 counteracts the inhibitory effects of hsa-miR-944 on breast cancer cell proliferation. (a, b) qRT-PCR analysis of HNRNPC expression in MDA-MB-231 (a) and MCF-7 (b) cells following transfection with si-circBACH2 alone, hsa-miR-944 inhibitor alone, or the combination of si-circBACH2 and hsa-miR-944 inhibitor. (c) Western blot analysis of HNRNPC protein levels in MDA-MB-231 and MCF-7 cells under the same transfection conditions. (d, f) CCK-8 assays showing cell proliferation of MDA-MB-231 (D) and MCF-7 (f) cells after transfection with si-circBACH2, hsa-miR-944 inhibitor, or their combination. (e, g) EdU incorporation assays indicating proliferating MDA-MB-231 (e) and MCF-7 (g) cells under the above conditions. *P < 0.05 versus siRNA negative control.

Regulation of BC progression by the circBACH2/hsa-miR-944/HNRNPC axis via the MAPK signaling pathway

Further experiments were conducted to explore the functional role of the circBACH2/hsa-miR-944/HNRNPC axis in breast cancer progression. Western blot analysis showed that inhibition of hsa-miR-944 significantly increased phosphorylation of ErK and MAPK in MDA-MB-231 and MCF-7 cells, while knockdown of circBACH2 reduced these phosphorylation levels. Notably, circBACH2 silencing effectively blocked the stimulatory effect of hsa-miR-944 inhibition on ErK and MAPK phosphorylation (**Figures 9a and 9b).** These findings indicate a strong negative correlation between circBACH2 and hsa-miR-944, as well as between hsa-miR-944 and phosphorylated ErK/MAPK. Collectively, these results suggest that upregulated circBACH2 acts as a sponge for hsa-miR-944 in the cytoplasm, enhancing HNRNPC expression and activity to promote BC cell proliferation, with the circBACH2/hsa-miR-944/HNRNPC axis mediating breast cancer progression through the MAPK signaling pathway **(Figure 9c).**

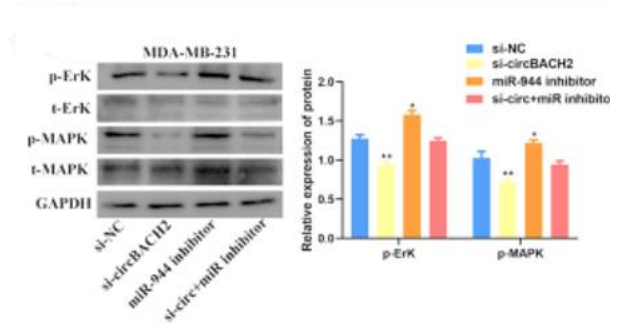

a)

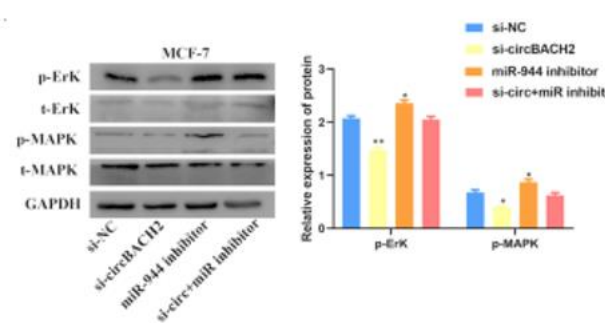

b)

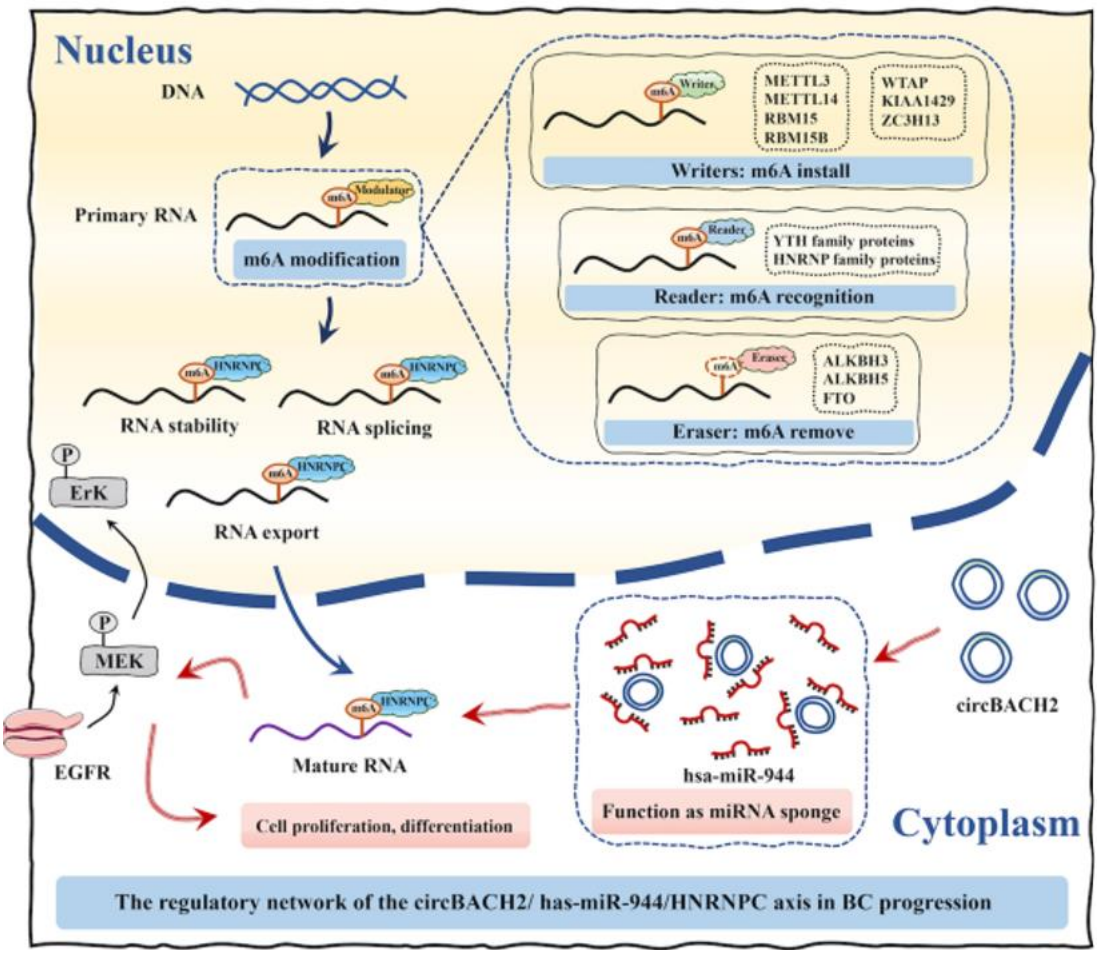

c)

Figure 9. Regulation of breast cancer progression by the circBACH2/hsa-miR-944/HNRNPC axis through the MAPK signaling pathway.

(a, b) Western blot analysis showing total ErK (t-ErK) and total MAPK (t-MAPK) protein levels, and phosphorylated ErK (p-ErK) and MAPK (p-MAPK) levels in MDA-MB-231 (a) and MCF-7 (b) cells after transfection with si-circBACH2 alone, hsa-miR-944 inhibitor alone, or their combination.

*P < 0.05 versus siRNA negative control.

(c) Schematic illustration of m6A modulators in RNA methylation and the potential regulatory mechanisms of the circBACH2/hsa-miR-944/HNRNPC axis in BC cell proliferation and progression.

Tumor cells acquire malignant phenotypes through a combination of genetic and epigenetic alterations, including modifications to mRNA transcripts. Among these, m6A methylation represents one of the most abundant RNA modifications in eukaryotic cells, influencing RNA processing, nuclear export, and translation. Accumulating evidence indicates that m6A modifications critically contribute to cancer development and progression. In this study, we focused on the role of m6A-related mechanisms in breast cancer and explored how circRNA–miRNA networks regulate m6A RNA methylation modulators.

We established a circRNA–m6A interaction network centering on the circBACH2/hsa-miR-944/HNRNPC axis in breast cancer. The hsa-miR-944/HNRNPC pair was associated with clinicopathological features and patient prognosis. Notably, circBACH2 acted as a sponge for hsa-miR-944, counteracting its inhibitory effect on HNRNPC expression, which in turn promoted breast cancer cell proliferation and progression.

Based on differential expression and prognostic analysis in TCGA datasets, RBM15B, HNRNPC, YTHDF3, and ZC3H13 were identified as key m6A RNA methylation modulators, with HNRNPC selected for constructing the regulatory network. m6A regulators have been shown to affect breast cancer prognosis. For example, Wang et al. reported dysregulation of m6A regulators in TNBC, with upregulation of KIAA1429, YTHDF2, and RBM15, and downregulation of ZC3H13, METTL14, and FTO [19, 20]. Gong et al. found that METTL14 and ZC3H13 mRNA levels were reduced in BC, suggesting their cooperative role in modulating proliferation, invasion, and metastasis [21]. YTHDF3, an m6A reader, is overexpressed in BC brain metastases and contributes to tumor progression via regulation of ST6GALNAC5, GJA1, EGFR, and VEGFA [22, 23]. HNRNPC, an RNA-binding protein, is highly expressed in BC and suppresses accumulation of immunostimulatory RNAs [24]. Our results corroborate the elevated expression of HNRNPC in BC, highlighting how dysregulation of m6A writers, readers, or erasers can drive malignant transformation.

miRNAs also play crucial roles in cancer pathogenesis. miR-944 exhibits dual functions depending on the tumor type. It acts as a tumor suppressor in colorectal cancer by targeting GATA6 [25], but has been reported as an oncogene in BC mediating chemoresistance [26]. Consistently, Flores-Pérez et al. observed that miR-944 is downregulated in BC cells regardless of hormone receptor status and stage, inhibiting migration and invasion [26]. In our study, miR-944 functioned as a tumor suppressor by restraining HNRNPC expression, aligning with the findings of Flores-Pérez et al. However, further studies are needed to fully elucidate the mechanistic roles of miR-944 in BC.

CircRNAs are widely expressed non-coding RNAs in eukaryotic cells, characterized by their stability, diversity, and evolutionary conservation. Emerging evidence indicates that circRNAs are dysregulated in breast cancer (BC) tissues and contribute to tumorigenesis by acting as miRNA sponges [27]. For example, Yang et al. identified 47 upregulated and 307 downregulated differentially expressed (DE) circRNAs to construct a competing endogenous RNA (ceRNA) network in BC [28]. Similarly, elevated circAGFG1 has been linked to enhanced cell proliferation and poor prognosis through a circRNA–miRNA–hub gene network in BC pathogenesis.

Despite numerous studies investigating the expression, function, and mechanisms of m6A RNA methylation regulators and their interaction with miRNAs in BC, the involvement of circRNAs in these regulatory axes remains poorly understood. Moreover, few reports have explored the functional roles of circRNA–miRNA–m6A modulator networks across BC stages or subtypes. Motivated by this gap, we explored the potential connection between circRNAs and m6A modification. Among candidate circRNAs, circBACH2 was selected due to its upregulation in triple-negative breast cancer (TNBC) tissues and association with malignant progression in TNBC patients [17]. Mechanistic studies have shown that circBACH2 functions as an oncogene in TNBC via the miR-186-5p/miR-548c-3p/CXCR4 axis. Furthermore, Cai et al. reported that in papillary thyroid carcinoma (PTC), circBACH2 sponges miR-139-5p to promote tumorigenesis via the circBACH2/miR-139-5p/LMO4 axis [18]. In our study, we demonstrated that circBACH2 enhances BC cell proliferation by sequestering hsa-miR-944, thereby upregulating HNRNPC expression and establishing a functional circRNA–miRNA–mRNA regulatory network. These results are consistent with prior studies indicating the oncogenic role of circBACH2 in BC development.

The MAPK signaling pathway is a well-known regulator of critical cellular processes associated with cancer, including proliferation, differentiation, apoptosis, and immune evasion [29]. Activation of this pathway has been reported to promote BC cell stemness and metastasis [30, 31]. Non-coding RNAs also participate in MAPK-mediated BC progression; for instance, miR-188 inhibits migration and induces apoptosis by suppressing MAPK activation via Rap2c regulation [32]. Based on these insights, we focused on the MAPK/ERK pathway to examine how the circBACH2/hsa-miR-944/HNRNPC axis drives BC cell proliferation. Western blot analysis revealed that inhibition of hsa-miR-944 increased ErK and MAPK phosphorylation, while circBACH2 knockdown reversed this effect, indicating that circBACH2 overexpression promotes MAPK pathway activation. These findings suggest that circBACH2 accelerates BC cell proliferation by acting as a hsa-miR-944 sponge to enhance HNRNPC expression, highlighting a previously unrecognized tumor-promoting mechanism in BC.

Conclusion

In summary, this study demonstrates that circBACH2 sponges hsa-miR-944 to elevate the expression of the

m6A RNA methylation modulator HNRNPC, thereby promoting BC progression. CircBACH2 functions as an oncogenic circRNA through the circBACH2/hsa-miR-944/HNRNPC axis, offering a potential novel target for BC diagnosis and therapy.

Acknowledgments: None

Conflict of Interest: None

Financial Support: None

Ethics Statement: None

1. Siegel RL, Miller KD, Jemal A. Cancer statistics, 2020. CA Cancer J Clin. 2020;70:7–30. doi: 10.3322/caac.21590
2. Yu F, Quan F, Xu J, Zhang Y, Xie Y, Zhang J, et al. Breast cancer prognosis signature: linking risk stratification to disease subtypes. Brief Bioinform. 2019;20:2130–2140. doi: 10.1093/bib/bby073
3. Yang Y, Hsu PJ, Chen Y-S, Yang Y-G. Dynamic transcriptomic m6A decoration: writers, erasers, readers and functions in RNA metabolism. Cell Res. 2018;28:616–624. doi: 10.1038/s41422-018-0040-8
4. Oerum S, Meynier V, Catala M, Tisné C. A comprehensive review of m6A/m6Am RNA methyltransferase structures. Nucleic Acids Res. 2021 doi: 10.1093/nar/gkab378
5. Xu X, Zhou E, Zheng J, Zhang C, Zou Y, Lin J, et al. Prognostic and predictive value of m6A "Eraser" related gene signature in gastric cancer. Front Oncol. 2021;11:1–10. doi: 10.3389/fonc.2021.631803
6. Liao S, Sun H, Xu C. YTH Domain: a family of N 6 -methyladenosine (m 6 A) Readers. Genomics Proteomics Bioinformatics. 2018;16:99–107. doi: 10.1016/j.gpb.2018.04.002
7. Dai XY, Shi L, Li Z, Yang HY, Wei JF, Ding Q. Main N6-methyladenosine readers: YTH family proteins in cancers. Front Oncol. 2021;11:1–11. doi: 10.3389/fonc.2021.635329
8. Jiang X, Liu B, Nie Z, Duan L, Xiong Q, Jin Z, et al. The role of m6A modification in the biological functions and diseases. Signal Transduct Target Ther. 2021;6:74. doi: 10.1038/s41392-020-00450-x
9. Li X, Yang L, Chen LL. The biogenesis, functions, and challenges of circular RNAs. Mol Cell. 2018;71:428–442. doi: 10.1016/j.molcel.2018.06.034
10. Chi F, Cao Y, Chen Y. Analysis and validation of circRNA-miRNA network in regulating m6A RNA methylation modulators reveals circMAP2K4/miR-139-5p/YTHDF1 axis involving the proliferation of hepatocellular carcinoma. Front Oncol. 2021;11:1–12. doi: 10.3389/fonc.2021.560506
11. Zhang B, Wu Q, Li B, Wang D, Wang L, Zhou YL. M6A regulator-mediated methylation modification patterns and tumor microenvironment infiltration characterization in gastric cancer. Mol Cancer. 2020;19:1–21. doi: 10.1186/s12943-019-1085-0
12. Jin Y, Wang Z, He D, Zhu Y, Hu X, Gong L, et al. Analysis of m6A-related signatures in the tumor immune microenvironment and identification of clinical prognostic regulators in adrenocortical carcinoma. Front Immunol. 2021;12:1–17. doi: 10.3389/fimmu.2021.637933
13. Shi H, Wei J, He C. Where, when, and how: context-dependent functions of RNA methylation writers, readers, and erasers. Mol Cell. 2019;74:640–650. doi: 10.1016/j.molcel.2019.04.025
14. Petri BJ, Klinge CM. Regulation of breast cancer metastasis signaling by miRNAs. Cancer Metastasis Rev. 2020;39:837–886. doi: 10.1007/s10555-020-09905-7
15. Hosonaga M, Saya H, Arima Y. Molecular and cellular mechanisms underlying brain metastasis of breast cancer. Cancer Metastasis Rev. 2020;39:711–720. doi: 10.1007/s10555-020-09881-y
16. Wada M, Canals D, Adada M, Coant N, Salama MF, Helke KL, et al. P38 delta MAPK promotes breast cancer progression and lung metastasis by enhancing cell proliferation and cell detachment. Oncogene. 2017;36:6649–6657. doi: 10.1038/onc.2017.274
17. Wang X, Xue B, Zhang Y, Guo G, Duan X, Dou D. Up-regulated circBACH2 contributes to cell proliferation, invasion, and migration of triple-negative breast cancer. Cell Death Dis. 2021;12:412. doi: 10.1038/s41419-021-03684-x
18. Cai X, Zhao Z, Dong J, Lv Q, Yun B, Liu J, et al. Circular RNA circBACH2 plays a role in papillary thyroid carcinoma by sponging miR-139-5p and regulating LMO4 expression. Cell Death Dis. 2019;10:184. doi: 10.1038/s41419-019-1439-y
19. Wang S, Zou X, Chen Y, Cho WC, Zhou X. Effect of N6-methyladenosine regulators on progression and prognosis of triple-negative breast cancer. Front Genet. 2021;11:580036. doi: 10.3389/fgene.2020.580036

20. Zhang B, Gu Y, Jiang G. Expression and prognostic characteristics of m6 A RNA methylation regulators in breast cancer. Front Genet. 2020;11:1–14. doi: 10.3389/fgene.2020.00001
21. Gong PJ, Shao YC, Yang Y, Song WJ, He X, Zeng YF, et al. Analysis of N6-methyladenosine methyltransferase reveals METTL14 and ZC3H13 as tumor suppressor genes in breast cancer. Front Oncol. 2020;10:1–18. doi: 10.3389/fonc.2020.00001
22. Chang G, Shi L, Ye Y, Shi H, Zeng L, Tiwary S, et al. YTHDF3 induces the translation of m6A-enriched gene transcripts to promote breast cancer brain metastasis. Cancer Cell. 2020;38:857–871.e7. doi: 10.1016/j.ccell.2020.10.004
23. Anita R, Paramasivam A, Priyadharsini JV, Chitra S. The m6A readers YTHDF1 and YTHDF3 aberrations associated with metastasis and predict poor prognosis in breast cancer patients. Am J Cancer Res. 2020;10:2546–2554
24. Sarbanes SL, Le Pen J, Rice CM. Friend and foe, HNRNPC takes on immunostimulatory RNAs in breast cancer cells. EMBO J. 2018;37:2–4. doi: 10.15252/embj.2018100923
25. Tang JT, Zhao J, Sheng W, Zhou JP, Dong Q, Dong M. Ectopic expression of miR-944 impairs colorectal cancer cell proliferation and invasion by targeting GATA binding protein 6. J Cell Mol Med. 2019;23:3483–3494. doi: 10.1111/jcmm.14245
26. Flores-Pérez A, Marchat LA, Rodríguez-Cuevas S, Bautista VP, Fuentes-Mera L, Romero-Zamora D, et al. Suppression of cell migration is promoted by miR-944 through targeting of SIAH1 and PTP4A1 in breast cancer cells. BMC Cancer. 2016;16:1–12. doi: 10.1186/s12885-016-2470-3
27. He X, Xu T, Hu W, Tan Y, Wang D, Wang Y, et al. Circular RNAs: their role in the pathogenesis and orchestration of breast cancer. Front Cell Dev Biol. 2021;9:1–17. doi: 10.3389/fcell.2021.647736
28. Yang R, Xing L, Zheng X, Sun Y, Wang X, Chen J. The circRNA circAGFG1 acts as a sponge of miR-195-5p to promote triple-negative breast cancer progression through regulating CCNE1 expression. Mol Cancer. 2019;18:1–19. doi: 10.1186/s12943-018-0930-x
29. Peluso I, Yarla NS, Ambra R, Pastore G, Perry G. MAPK signalling pathway in cancers: olive products as cancer preventive and therapeutic agents. Semin Cancer Biol. 2019;56:185–195. doi: 10.1016/j.semcancer.2017.09.002
30. Lv Y, Wang X, Li X, Xu G, Bai Y, Wu J, et al. Nucleotide de novo synthesis increases breast cancer stemness and metastasis via cGMP-PKG-MAPK signaling pathway. PLoS Biol. 2020;18:1–24. doi: 10.1371/journal.pbio.3000872
31. Wen S, Hou Y, Fu L, Xi L, Yang D, Zhao M, et al. Cancer-associated fibroblast (CAF)-derived IL32 promotes breast cancer cell invasion and metastasis via integrin β3–p38 MAPK signalling. Cancer Lett. 2019;442:320–332. doi: 10.1016/j.canlet.2018.10.015
32. Zhu X, Qiu J, Zhang T, Yang Y, Guo S, Li T, et al. MicroRNA-188-5p promotes apoptosis and inhibits cell proliferation of breast cancer cells via the MAPK signaling pathway by targeting Rap2c. J Cell Physiol. 2020;235:2389–2402. doi: 10.1002/jcp.29144